European Journal of Medicinal Chemistry 44 (2009) 981–989

Contents lists available at ScienceDirect

European Journal of Medicinal Chemistry

journal homepage: http://www.elsevier.com/locate/ejmech

Original article

Synthesis of novel benzo[*h*]quinolines: Wound healing, antibacterial, DNA binding and in vitro antioxidant activity

Halehatty R. Prakash Naik [a], Halehatty S. Bhojya Naik [a,*], Thangali R. Ravikumar Naik [a], H. Raja Naika [b], K. Gouthamchandra [b], Riaz Mahmood [b], B.M. Khadeer Ahamed [c]

[a] *Department of Studies and Research in Industrial Chemistry, School of Chemical Sciences, Kuvempu University, Shankaraghatta, Bhadravati Taluk 577 451, Shimoga, Karnataka, India*
[b] *Department of Studies and Research in Biotechnology, School of Biological Sciences, Kuvempu University, Shankaraghatta 577 451, Karnataka, India*
[c] *Department of Studies and Research in Biochemistry, Basaveshwara Medical College, Chitradurga, Karnataka, India*

ARTICLE INFO

Article history:
Received 27 February 2008
Received in revised form 27 June 2008
Accepted 8 July 2008
Available online 16 July 2008

Keywords:
Sulfur/selenium-benzo[*h*]quinolines
Wound healing activity
Antibacterial
DNA binding
In vitro antioxidant activity

ABSTRACT

We have characterized a new class of 2-mercapto/2-selenobenzo[*h*]quinoline-3-carbaldehyde (**3**/**4**). Antibacterial potential of these compounds against a wide range of Gram-positive and Gram-negative bacteria was studied. The selenium containing compound **4** showed significant inhibition zone on *Staphylococcus aureus* (22.76 ± 0.14), *Bacillus subtilis* (20.63 ± 0.24), and *Streptococcus pyogenes* (19.54 ± 0.20) over sulfur containing compound **3**. To validate the ethnotherapeutic claims of the synthetic compounds in skin diseases, wound healing activity was studied, besides antioxidant activity to understand the mechanism of wound healing. The interaction behavior of these compounds with DNA was investigated by absorption spectra (obtained K_b constant for **3** is 2.7×10^5 and for **4** is 3.8×10^6), viscosity, and thermal denaturation studies. Finally, the results show that the DNA intercalated **3**/**4** compounds are strong antioxidants; they show significan wound healing activity and protect oxidative DNA damage from harmful free radical reactions.

1. Introduction

It is well known that the quinoline ring system is an important structural unit widely existing in alkaloids, therapeutics and synthetic analogues with interesting biological activities [1–3]. A large variety of quinoline derivatives have been used as antimalarial, anti-inflammatory, antiasthmatic, antibacterial, antihypertensive and platelet derived growth factor receptor tyrosine kinase (PDGF-RTK) inhibiting agents [4,5].

Recent studies reveal that the intramolecularly stabilized organoselenium and sulfur compounds play an important role in the catalytic antioxidant activity [6,7]. Since, Se resembles sulfur (S) in many of its properties, it is isosteric [8,9]. The biological and pharmaceutical activities of different selenium compounds are of special interest because they are active sites of a large number of selenium dependent enzymes, such as glutathione peroxidase (GSHPx) [10,11] and help in prevention of cancer [12]. In the same field of research, results of many studies [13,14] have related Se deficient bioavailability and intake to human cancer mortality. New synthetic selenium compounds may provide a way to minimize toxicity associated with higher selenium intake. Recently, several forms of organoselenium have been studied for their cancer preventive activities. The dietary *p*-methoxybenzeneselenol, a synthetic organoselenium compound, was found to inhibit azoxymethane-induced hepatocarcinogenesis in rats without clinical signs of toxicity [15].

Wounds are physical injuries that result in an opening or breaking of the skin. Proper healing of wounds is essential for the restoration of disrupted anatomical continuity and disturbed functional status of the skin. It is a product of the integrated response of several cell types to injury. Wound healing is a complex multifactorial process that results in the contraction and closure of the wound and restoration of a functional barrier [16]. Repair of injured tissues occurs as a sequence of events, which include inflammation, proliferation and migration of different cell types [17]. It is consented that reactive oxygen species (ROS) are deleterious to wound healing process due to the harmful effects on cells and tissues. Absorbable synthetic biomaterials are considered to be degraded via ROS [18]. Free-radical-scavenging enzymes (FRSE) belong to a cytoprotective enzymal group that has an essential role in the reduction, deactivation and removal of ROS as well as regulating the wound healing process. These cells, through their characteristic "respiratory burst" activity, produce free radicals [19]. Wound related non-phagocytic cells also generate free radicals by involving non-phagocytic NADPH oxidase mechanism [20].

* Corresponding author. Fax: +91 8282 256255.
E-mail address: hsb_naik@rediffmail.com (H.S.B. Naik).

0223-5234/$ – see front matter © 2008 Elsevier Masson SAS. All rights reserved.
doi:10.1016/j.ejmech.2008.07.006

Topical applications of compounds with free-radical-scavenging properties in patients have shown to improve wound healing significantly and protect tissues from oxidative damage [21].

Demonstration of potential antioxidant activity of heterocyclic compounds with DNA is of major biochemical and biological importance [22]. It has been suggested that quinolines can chelate Fe(II) and Fe(III) and prevent free radical production in Fenton reaction [23] and quinolines can also intercalate DNA duplex and react with free radicals in order to protect DNA from oxidative damage; covalent bindings of quercetin to DNA and protein have been recently reported [24–26].

In this context, antibacterial potential of our synthesized compounds against a wide range of Gram-positive and Gram-negative bacteria was studied with six bacterial strains. To validate the ethnotherapeutic claims of these S/Se compounds in antibacterials, wound healing activity was studied, and in addition DNA binding and in vitro antioxidant activity were also studied.

2. Results and discussion

2.1. Chemistry

The synthetic methodologies that have been used to create the benzo[*h*]quinoline nucleus are generally adaptations of the commonly used methods of quinoline synthesis (e.g. Skraup, and Doebner and Von Miller) [27–30], although other routes involving Diels–Alder reactions [31] and Friedlander condensations [32] provide alternative, multistep approaches. We have used the Vilsmeier reaction previously to access a variety of 2,3-substituted and 2,3-fused quinolines [33,34] by reacting *N*,*N*-dimethylformamide (DMF) with an appropriate *N*-arylacetamide in the presence of phosphorus oxychloride ($POCl_3$). Acetylation of α-naphthylamine provided an alternative nucleophilic species (**1**) which reacted with DMF under the same conditions to offer 2-chlorobenzo[*h*]quinoline-3-carbaldehyde (**2**) (Scheme 1). This appropriately substituted heterocycle along with the corresponding 3,4-substituted benzo[*h*]quinoline [35] was recognized as a potential precursor to analogues of a number of agents with anticancer activity [36,37].

Thus, the chlorine group of 2-chlorobenzo[*h*]quinoline-3-carbaldehyde was replaced according to our reported procedures [38–42]. The appearance of singlet (that belongs to SH and SeH) in ^{1}H NMR spectra at δ 11.5 and 12.7 in both **3** and **4** confirms the replacement of chlorine in 2-position by SH and SeH. The shift of absorption frequencies in IR spectra at 1668 cm^{-1}, 1671 cm^{-1} of CHO and absence of 658 cm^{-1} (C–Cl) in contrast to newly appearing absorption bands at 2593 cm^{-1} and 3605 cm^{-1} in both **3** and **4** shows the formation of desired molecule. Finally, the structure was confirmed by its mass spectrum through the appearance of molecular ion peak at *m*/*z*: 216 [M^+] for **3** and 263 [M^+] for **4**.

2.2. Wound healing activity

Wound healing process consists of different phases such as granulation, collagenation, collagen maturation and scar maturation which are concurrent but independent to each other. Hence, in this study two different models were used to assess the effect of newly synthesized compounds containing ointment base (containing white bee wax, hard paraffin, cetyl alcohol and white soft paraffin) prepared by fusion method [43] on various phases.

The percentage of wound contraction was determined using the following formula:

$$\text{Percent of wound contraction} = \frac{\text{Healed area}}{\text{Total wound area}} \times 100$$

Wound area was measured by tracing the wound margin using a transparent paper each day with an interval of four days and healed area calculated by subtracting from the original wound area. On day 4, the wound contraction of standard and compound **4** ointment treated groups was found to be significant ($P < 0.001$) in comparison to simple ointment base treated group. On 16th day, standard ointment treated wound was completely healed while wound of compound **4** ointment treated group was also almost at complete healing stage. On day 18, wound of compound **3** ointment treated group healed 100% and simple ointment base treated group showed 95.71% healing. It was also observed that the epithelialization period of treated and standard groups was less in comparison to simple ointment base treated group (Table 1).

In the excision and incision wound repair model (Tables 1 and 2), the animals treated with newly synthesized compound **4** showed faster epithelialization than those treated with newly synthesized compound **3** and control. However, the topical treatment with positive control (1% w/w nitrofurazone gel) was found to be superior to all other treatments as evidenced by lesser number of days required for complete epithelialization of excision wounds and increased tensile strength of incision wounds (Fig. 1).

2.3. Antibacterial activity

The minimal inhibitory concentrations (MICs) of the newly synthesized compounds **3**, **4** and standard ciprofloxacin against all bacterial strains are as shown in Table 5. The significant MIC value was obtained for *Staphylococcus aureus*, 11 μg/mL for compound **3** and 8 μg/mL for compound **4**. Comparison of results of the antibacterial activity between newly synthesized compounds **3** and **4** and ciprofloxacin showed a synchronizing effect on strains of pathogenic bacteria. The zones of inhibition of the bacterial colony are depicted in Table 3. Compound **3** demonstrated antibacterial activity against all the strains of bacteria. But it is significant on Gram-positive bacteria *S. aureus* (19.40 mm) and *Streptococcus pyogenes* (17.41 mm). Among the two newly synthesized compounds, compound **4** containing selenium component proved to be a more potent bactericidal agent against *S. aureus* (22.76 mm), *S. pyogenes* – NCIM-2608 (19.54 mm) and *Bacillus subtilis* – NCIM-2010 (20.63 mm). Compound **3** containing sulfur showed a meager antimicrobial property against all the pathogenic strains of bacteria (Fig. 2).

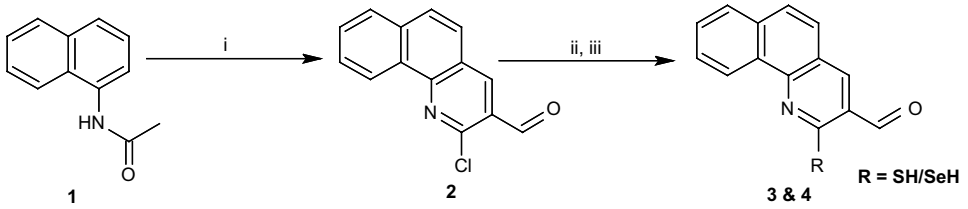

Scheme 1. Synthesis of 2-mercapto/selenobenzo[*h*]quinoline-3-carbaldehyde (**3**/**4**). (i) DMF/$POCl_3$ reflux; (ii) Na_2S reflux; (iii) NaHSe reflux.

Table 1
Effect of **3** and **4** on %wound closure of excision wound

Groups	Day 4	Day 8	Day 12	Day 16	Epithelization period (days)
I	42.66 ± 1.15	63.75 ± 0.94	77.31 ± 0.79	84.54 ± 0.24	24
II	55.68 ± 1.02*	87.21 ± 0.99*	97.68 ± 0.10*	100*	14
III	45.35 ± 1.17*	75.63 ± 0.94*	85.94 ± 0.78*	96.24 ± 0.14*	18
IV	53.65 ± 1.23*	85.26 ± 0.72*	95.70 ± 1.12*	100*	16
F-value	137	634	433	287	

Group I – control, group II – reference, group III – **3**, group IV – **4**. Values are mean ± S.E.; *$P < 0.01$ vs. control; $n = 6$ albino rats per group, tabular value represents mean ± S.E. *$P < 0.001$ (comparison of I with II, III and IV).

The results obtained in this study indicate a considerable difference in antibacterial activity among the two newly synthesized compounds. Compound **4** containing selenium exhibited significant antibacterial activity against pathogenic bacterial strains. Its bio-controlling potency is par with that of the standard antibiotic ciprofloxacin. Generally, the Gram-positive bacteria are more susceptible having only an outer peptidoglycan layer which is not an effective permeability barrier [44] whereas the Gram-negative bacteria possess an outer phospholipidic membrane carrying the structural lipopolysaccharide components. This makes the cell wall impermeable to drug constituents [45]. So the maximum inhibitory activity was observed in Gram-positive bacteria *S. aureus* and *S. pyogenes.* In the case of Gram-negative *Pseudomonas aeruginosa* and *Klebsiella pneumoniae* the zone of inhibitory activity was significant because of a multilayered phospholipidic membrane carrying the structural lipopolysaccharide components [46]. Selenium containing compound **4** showed maximum inhibition zones compared to that of sulfur containing compound **3**. Thus, compound **4** is effective in controlling the growth of pathogenic strains to a considerable extent. The highest activity of compound **4**, when compared to that of compound **3**, indicated that it was solely responsible for antibacterial activity.

2.4. DNA binding studies (absorption spectral studies)

Primarily, the DNA binding was observed by the following parameters: (i) electrostatic interactions with the negative charged nucleic sugar–phosphate structure which are along the external DNA double helix and do not possess selectivity; (ii) binding interactions with two grooves of DNA double helix; and (iii) intercalation between the stacked base pairs of native DNA.

Our parent compound's intercalation was evident from the major reduction in the intensity of UV–vis bands characteristic of quinolines upon DNA interaction (Fig. 3). A 20.3% and 18.2% of reduction in absorption observed at 293 nm (**3**) and 312 nm (**4**) is indicative of DNA–drug intercalation (Fig. 3). It has been demonstrated that intercalation of **3** and **4** into DNA duplex causes major reduction in the intensity of the UV–vis absorption band characteristic of compounds. This hypochromic shift indicates helical ordering of **3** and **4** in the DNA helix. The limitation on molecular movements of both compounds causes a decrease in its ability to absorb light energy [47,48]. Absorption spectral results exhibit hypochromism of about 20.5% and 25.1%, for compounds **3** and **4**, respectively (Table 4).

Table 2
Effect of synthesized compounds **3** and **4** on tensile strength of incision wounds

Groups	Tensile strength (g)
I	450.67 ± 4.09
II	599.00 ± 0.81*
III	544.83 ± 2.92*
IV	582.33 ± 1.44*
F-value	471

Group I – control, group II – reference, group III – **3**, group IV – **4**; values are mean ± S.E., *$P < 0.01$ vs. control; $n = 6$ albino rats per group, tabular value represents mean ± S.E. *$P < 0.001$ (comparison of I with II, III and IV).

2.5. Viscosity measurements

To further clarify the interaction modes of **3** and **4** with DNA were investigated by viscosity measurements. An increase in viscosity of native DNA is regarded as a diagnostic feature of an intercalation process [49,50]. We have measured the viscosity changes in short, rod-like DNA fragments. The relative length increase (L/L_0) of the complex formed between **3**/**4** and DNA is shown in Fig. 4. It is evident that binding of **3**/**4** increased the viscosity of DNA corresponding to an increase in the contour length of the DNA fragments. The measured slope of the plot 1.26 ± 0.03 falls within 63% (**4**) and 1.09 ± 0.025 falls within 54% (**3**) of the slope of a theoretical curve for an idealized intercalation process $(1 + 2r)$ [51,52]. On this basis we calculate that intercalation of **4** with DNA provoked an increase of 1.9 Å contour length of DNA. Since the size of these sonicated fragments was significantly greater than the persistent length (Fig. 4).

2.6. Thermal denaturation

Other strong evidence for the intercalative binding of **3**/**4** into the double helix DNA was obtained from DNA melting studies. The intercalation of small molecules into the double helix is known to increase the DNA melting temperature (T_m), at which the double helix denatures into single stranded DNA, owing to the increased stability of the helix in the presence of an intercalator [53]. The molar extinction coefficient of DNA bases at 260 nm in the double helical form is much less than the single stranded form; hence, melting of the helix leads to an increase in the absorbance at 260 nm [54]. Thus, the helix to coil transition temperature can be determined by monitoring the absorbance of DNA at 260 nm as a function of temperature. The DNA melting studies were carried out with calf thymus DNA in the absence and presence of **3**/**4** [1:5 ratio of **3** and **4** to DNA-c(P)]. T_m for calf thymus DNA was 60 ± 5 °C in the absence of compounds, but in the presence of **3**/**4**, the T_m of CT-DNA increased by 5 °C and 3 °C, respectively. The advantage of this method is that it is much easier to identify when more than one transition occurs [55]. These variations in DNA melting temperature strongly supported the intercalation of **3**/**4** into the double helix DNA (Fig. 5).

2.7. In vitro antioxidant activities

2.7.1. Superoxide anion scavenging activity

In the phenazine methosulfate (PMS)–nicotinamide adenine dinucleotide (NADH)–nitroblue tetrazolium (NBT) system, superoxide anion derived from dissolved oxygen by PMS–NADH coupling reaction reduces NBT. The antioxidant properties of the synthesized compounds were verified by their catalytic activities in the dismutation of superoxide radicals. The selenium containing

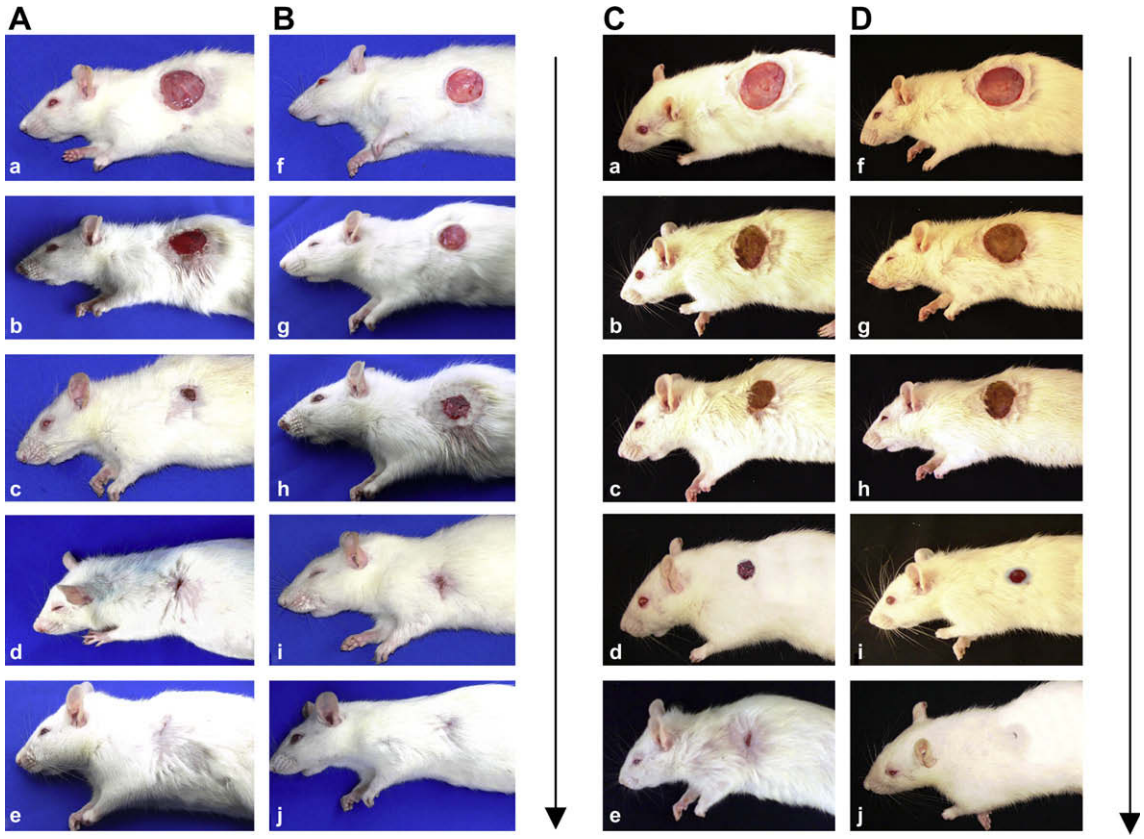

Fig. 1. Comparison of wound healing activity on group of rats: (A) wound healing activity by standard nitrofurazone drug containing ointment; (B) wound activity of compound **3**; (C) wound healing activity by cream base ointment; (D) wound activity of compound **4**.

compound 4 showed to be active catalysts, with a better performance of scavenging ability than **3**. The SOD activity of these molecules was compared with standard butylated hydroxytoluene (BHT) and butylated hydroxyanisole (BHA). The decrease of absorbance at 570 nm of **3** and **4** indicates the consumption of superoxide anion in the reaction mixture. Thus compounds possess stronger superoxide radical scavenging activity than butylated hydroxytoluene (BHT) and butylated hydroxyanisole (BHA) (Fig. 6).

The results were found to be statistically significant ($P < 0.05$), the percentage inhibition of superoxide generated by 60 μg/mL concentration of complexes was found to be 65% for **3** and 76% for **4**, which is greater than that of butylated hydroxytoluene (BHT) (51%) but less than butylated hydroxyanisole (BHA) (81%), respectively, at same concentration.

2.7.2. Scavenging of hydrogen peroxides

Hydrogen peroxide itself is not very reactive, but it can be toxic as sometimes it may give rise to a hydroxyl radical [56]. Thus, removing H_2O_2 is very important for the protection of biological systems. The synthesized compounds **3** and **4** are capable of scavenging hydrogen peroxide in a concentration-dependent manner was determined according to the method [57]. The scavenging ability of complexes and their ligands on hydrogen peroxide is shown in Fig. 5. At 60 μg/mL concentration complexes **3** and **4** exhibited 68% and 74% of scavenging effect over hydrogen peroxide, respectively, this difference might be due to the presence of selenium in **4**. Thus, statistically these results are significant and followed the order BHA > **3** > **4** > BHT for inhibition of hydrogen peroxide (Fig. 7).

Table 3
Antibacterial activity of the synthesized compounds against pathogenic bacterial strains

Clinical strains	Diameter of zone of inhibition (mm)		
	Compound **3**	Compound **4**	Ciprofloxacin
Pseudomonas aeruginosa	11.58 ± 0.21	12.23 ± 0.02	23.30 ± 0.20
Klebsiella pneumoniae	13.63 ± 0.17	14.46 ± 0.14	20.10 ± 0.20
Escherichia coli	12.31 ± 0.10	17.20 ± 0.34	19.25 ± 0.19
Staphylococcus aureus	19.40 ± 0.28	22.76 ± 0.14	21.38 ± 0.10
Streptococcus pyogenes	17.41 ± 0.10	19.54 ± 0.20	20.81 ± 0.20
Bacillus subtilis	15.25 ± 0.20	20.63 ± 0.24	21.30 ± 0.11
F-value	289.28	381.44	154.31

2.7.3. Free radical 1,1-diphenyl-2-picryl-hydrazyl (DPPH) scavenging activity

The reduction capability of DPPH radicals was determined by decrease in its absorbance at 517 nm. This decrease in absorbance of DPPH radical caused by antioxidants because of the reaction between **3** and **4** with DPPH radicals progresses, which results in the scavenging of the radical by hydrogen donation. It is visually noticeable as a discoloration. Hence, DPPH is an important substrate to evaluate antioxidant activity [58,59]. Fig. 8 illustrates significant ($P < 0.01$) decrease in the concentration of DPPH radical due to the scavenging ability of **3** and **4** compared to standards. The results indicate that the selenium containing compound **4** showed stronger DPPH scavenging activity rather than sulfur containing compound **3**. Statistically, the scavenging effect of compounds with DPPH radical decreased in the following order BHA > **4** > **3** > BHT with 64%, 61%, 55%, and 48% of inhibition, respectively (Fig. 8).

2.7.4. Reducing power

The reducing capacity of both compounds **3** and **4** may serve as a significant indicator of its potential antioxidant activity [60]. The antioxidant activity of putative antioxidants has been attributed to

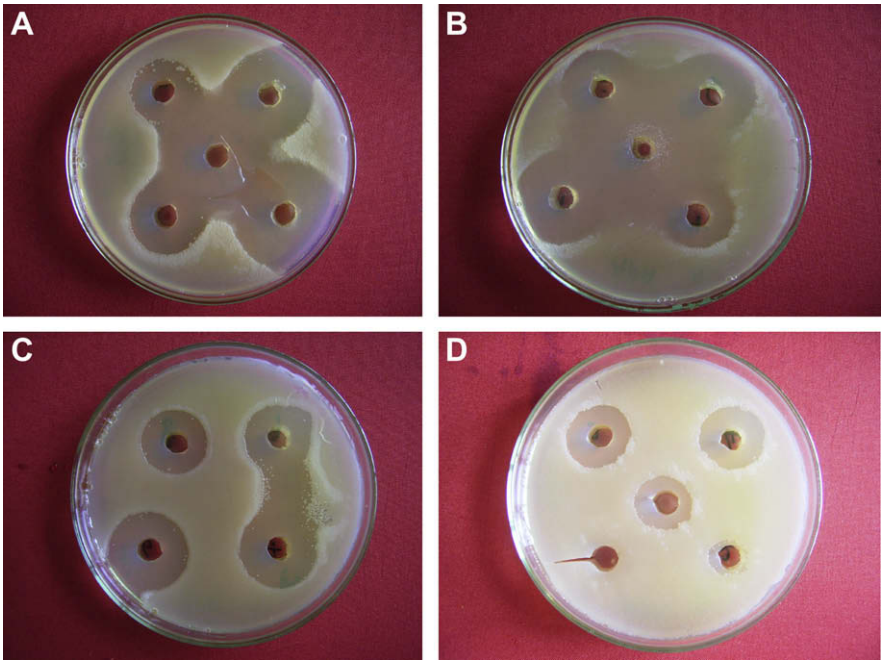

Fig. 2. Antibacterial activity of compound **4**. A: zone of inhibition for *Staphylococcus aureus*; B: zone of inhibition for *Bacillus subtilis*; C: zone of inhibition for *Streptococcus pyogenes*; D: zone of inhibition for *Escherichia coli*.

various mechanisms, among which are prevention of chain initiation, binding of transition metal ion catalysts, decomposition of peroxides, prevention of continued hydrogen abstraction, reductive capacity, and radical scavenging. The reducing power of **3**/**4** increased with decrease in absorbance value. Compound **4** exhibited stronger reducing power than compound **3**, may be due to the presence of selenium/sulfur in **4**/**3** but this difference between compounds was found statistically significant ($P > 0.06$) with standard compounds following the order: BHA > **4** > **3** > BHT which is shown in Fig. 9.

3. Conclusion

In conclusion, we developed a versatile and useful new access to different scaffold of biologically importance 2-mercapto/2-selenobenzo[*h*]quinoline-3-carbaldehyde. On the basis of the results, it is clearly indicated that the newly synthesized compounds have significant antioxidant activity against various in vitro antioxidant systems. Further, it shows that they bind DNA via intercalative modes and are strong antioxidants which protect DNA from harmful chemical reactions. Therefore, it is suggested that further work could be performed on similar benzo[*h*]quinoline analogues as antioxidants and wound healing agents.

4. Experimental

4.1. Chemicals

All reagents and solvents used were of AR grade, commercially purchased. Ferric chloride, 1,1-diphenyl-2-picryl-hydrazyl (DPPH), nicotinamide adenine dinucleotide (NADH), butylated hydroxyanisole (BHA), butylated hydroxytoluene (BHT), and trichloroacetic acid (TCA) were purchased from Sigma (Sigma–Aldrich, E. Merck, Himedia, Qualigens, Mumbai, India), Calf thymus DNA

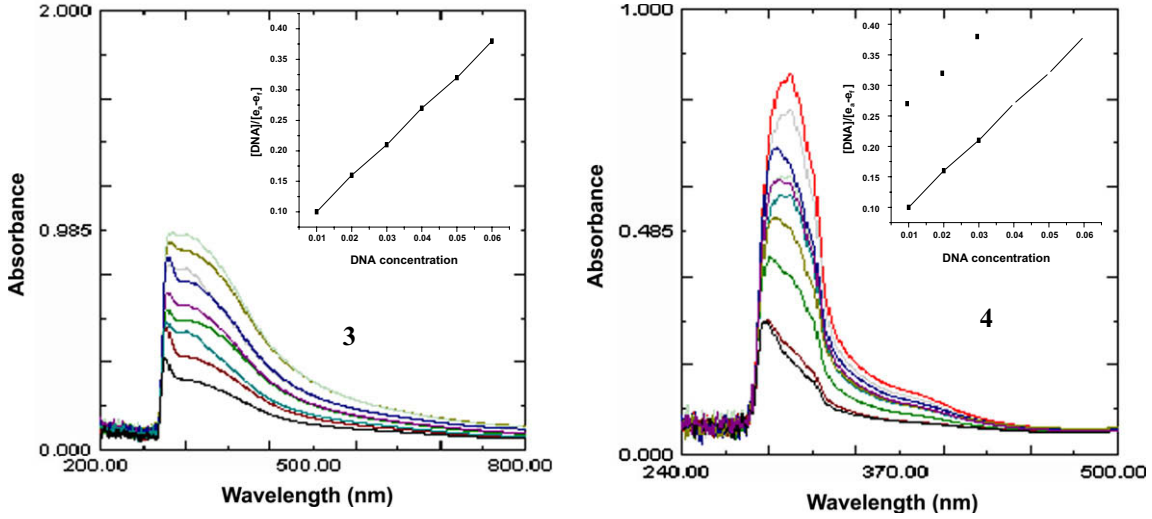

Fig. 3. (A) Absorption spectra for **3**/**4** in Tris–HCl buffer upon addition of DNA. Compound **3**/**4** = 0.5 μM, [DNA] = 0–100 μM. (B) Inner graph of $[DNA]/(\varepsilon_a - \varepsilon_f)$ vs. [DNA] for titration of DNA with **3**/**4**.

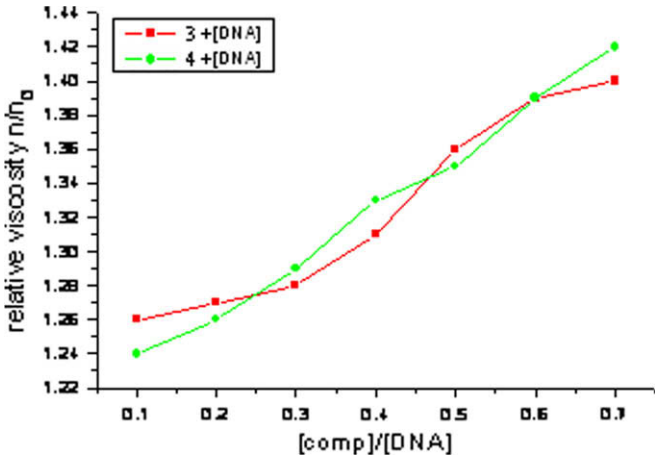

Fig. 4. Effect of **3**/**4** on the viscosity of CT-DNA at 25 ± 0.1 °C. Compound **3**/**4** = 0–100 μM and [DNA] = 50 μM.

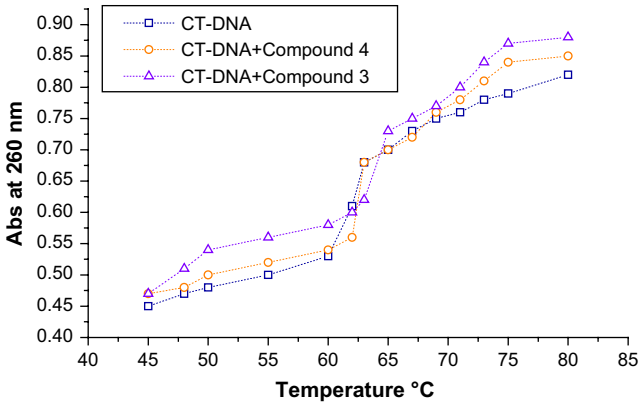

Fig. 5. Melting curves of CT-DNA in the absence and presence of **3**/**4**.

(CT-DNA) was purchased from Bangalore Gene, Bangalore, India and solution was prepared using deionised double distilled water. Melting points were determined in an open capillary tube and are uncorrected. IR spectra were recorded in KBr pellets on Perkin–Elmer 157 IR spectrophotometer. ^{1}H NMR spectra were recorded in DMSO-d_6 on EM-390 (300 MHz) NMR spectrometer. Mass spectra were recorded on MASPEC low resolution instrument operating at 70 eV and UV–vis spectra were recorded using SHIMADZU, UV-1650 PC model.

4.2. Synthesis of 2-mercaptobenzo[h]quinoline-3-carbaldehyde (**3**)

A mixture of 2-chlorobenzo[*h*]quinoline-3-carbaldehyde **2** (1.58 g, 1 mmol) and Na_2S (1 g, 1 mmol) was refluxed in ethanol (25 mL) for 2–3 h in the presence of 6–8 mL of conc. HCl. The completion of the reaction was monitored by TLC, eluting the phase with ethyl acetate:carbon tetrachloride (70:30). The reaction mixture was poured into crushed ice (50 g). The product was filtered, washed with distilled water, dried and recrystallised with methanol.

Pale yellow solid, yield 85%, m.p. 243 °C; IR (ν) (KBr) cm^{-1}: 3015 (C–H, Ar-H); 1668 (CHO); 2593 (S–H); ^{1}H NMR (DMSO-d_6) δ: 7.68 (d, 1H, Ar-H, J = 8.03), 7.32 (d, 1H, Ar-H, J = 7.63), 7.34 (d, 1H, Ar-H, J = 7.45), 7.69 (d, 1H, Ar-H, J = 7.37), 7.44 (d, 1H, Ar-H, J = 7.45), 7.70 (d, 1H, Ar-H, J = 7.45), 8.30 (d, 1H, Ar-H, J = 7.45), 9.67 (d, 1H, CHO), 11.5 (d, 1H, C–SH); MS: m/z 239 [M]$^+$; elemental analysis: found: C, 70.28; H, 3.78; N, 5.86. Calculated for $C_{14}H_9NOS$: C, 70.27; H, 3.79; N, 5.85.

4.3. Synthesis of 2-selenobenzo[h]quinoline-3-carbaldehyde (**4**)

A mixture of 2-chlorobenzo[*h*]quinoline-3-carbaldehyde **2** (1.58 g, 1 mmol) and NaHSe (1 g, 1 mmol) was refluxed at 80–90 °C in the presence of ethanol (5 mL) for 1 h. The completion of the reaction was monitored by TLC, eluting the phase with ethyl acetate:carbon tetrachloride (80:20). The reaction mixture was poured into crushed ice (25 g). The product was filtered, washed with distilled water, dried and recrystallised with methanol.

Table 4
Intrinsic binding constants (K_b) and DNA melting temperature (T_m)

Compound	K_b(M^{-1})	T_m (°C)
3	2.7×10^5	60
4	3.8×10^6	58

Brown solid, yield 63%, m.p. 265 °C; IR (ν) (KBr) cm^{-1}: 3019 (C–H, Ar-H); 1671 (CHO); 2605 (Se–H); ^{1}H NMR (DMSO-d_6) δ: 7.67 (d, 1H, Ar-H, J = 7.65), 7.34 (d, 1H, Ar-H, J = 7.64), 7.33 (d, 1H, Ar-H, J = 7.45), 7.68 (d, 1H, Ar-H, J = 7.47), 7.13 (d, 1H, Ar-H, J = 7.45), 7.15 (d, 1H, Ar-H, J = 7.45), 8.22 (d, 1H, Ar-H, J = 7.63), 9.69 (d, 1H, CHO), 12.7 (d, 1H, C–SeH). MS: m/z 286 [M]$^+$; elemental analysis: found: C, 58.75; H, 3.19; N, 4.91. Calculated for $C_{14}H_9NOSe$: C, 58.76; H, 3.17; N, 4.89.

4.4. Wound healing activity

4.4.1. Animals

Male Wistar rats weighing 200–250 g were used. They were kept in a standard environmental condition and fed with rodent diet and water ad libitum.

In the experiment, the rats were divided into four groups (n = 6): group one was the control group which received simple ointment base, group two was treated with reference standard (0.2% w/w nitrofurazone ointment) and groups three and four received our newly synthesized compounds **3** and **4** containing cream base ointment (100/500 mm^2) topically on wound created on the dorsal back of rats daily till the wounds completely healed [61].

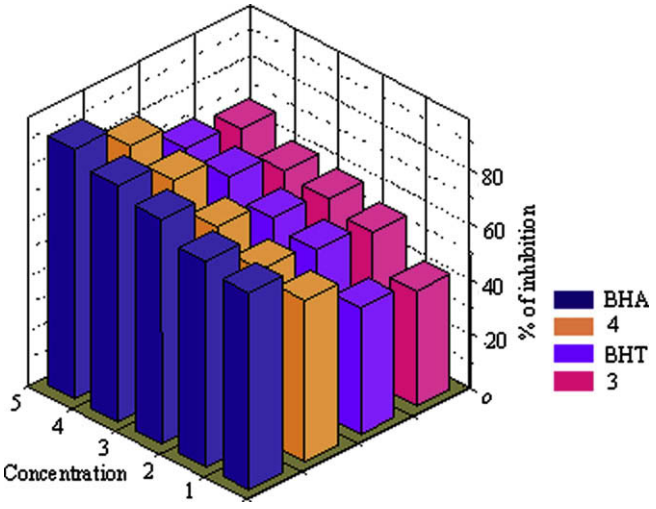

Fig. 6. Superoxide anion radical scavenging activity of **3**/**4** with BHA, and BHT by the PMS–NADH–NBT method (BHA: butylated hydroxyanisole, BHT: butylated hydroxytoluene).

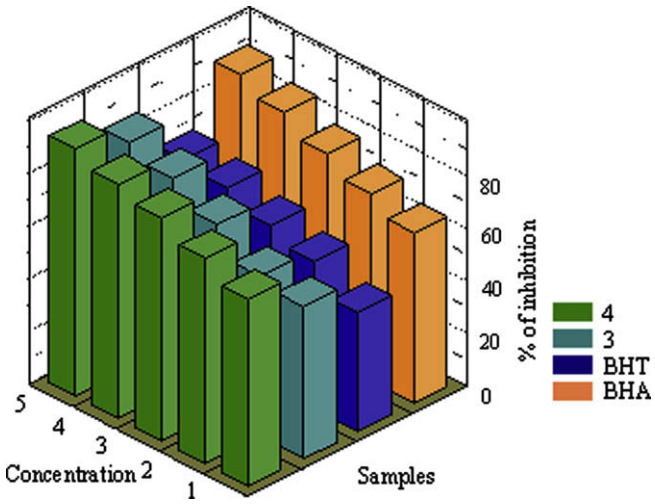

Fig. 7. Percentage of inhibition plot for H_2O_2 scavenging activity in presence of **3**/**4** against standard BHA, and BHT.

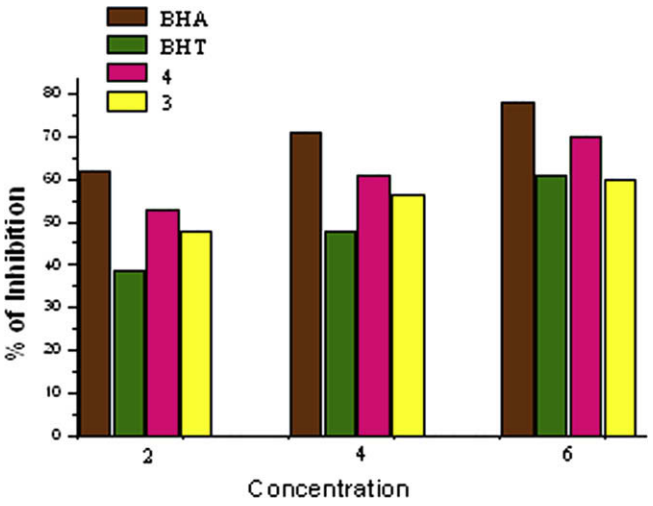

Fig. 9. Bar graph showing the percentage of inhibition of reducing power of compound **3**/**4** with BHA, and BHT.

4.4.2. Excision wound model

Full thickness excision wound was made on the shaved back of the rat by removing a 500 mm^2 piece of skin and the day on which wound was made was considered as day zero [62]. Animals divided into four groups were treated as described above. The percent of wound closure was recorded on days 4, 8, 12 and 16 and the wound area was traced and measured planimetrically. The actual value was converted into percent value taking the size of the wound at the time of wounding as 100%.

4.4.3. Incision wound model

Experimental rats were anaesthetized and two paravertebral-long incisions were made through the skin and cutaneous muscles at a distance of about 1.5 cm from the midline on each side of the depilated back of the rat. Full aseptic measures were not taken and no local or systemic antimicrobial was used throughout the experiment [63].

All the groups were treated in the same manner as mentioned in the case of the excision wound model. No ligature was used for stitching. After the incision was made, the parted skin was kept together and stitched with black silk at 0.5 cm intervals. Surgical thread (no. 000) and a curved needle (no. 11) were used for stitching. The continuous thread on both wound edges was tightened for good closure of the wounds. The wound was left undressed, compounds **3** and **4** cream base ointments, along with water-soluble base ointment (control) and nitrofurazone ointment were applied topically twice a day for 9 days. When wounds were cured the sutures were removed on the 9th day and tensile strength was measured with a tensiometer.

The tensile strength of a wound represents the degree of wound healing. Usually wound healing agents promote a gain in tensile strength. The sutures were removed on the 9th day after wounding and the tensile strength was measured on the 10 day. The herbal ointment along with standard and control was applied throughout the period, twice daily for 9 days. The mean tensile strength on the two paravertebral incisions on both sides of the animals was taken as the measures of the tensile strength of the wound for an individual animal. The tensile strength of wounds treated with ointment containing compounds **3**/**4** was compared with control.

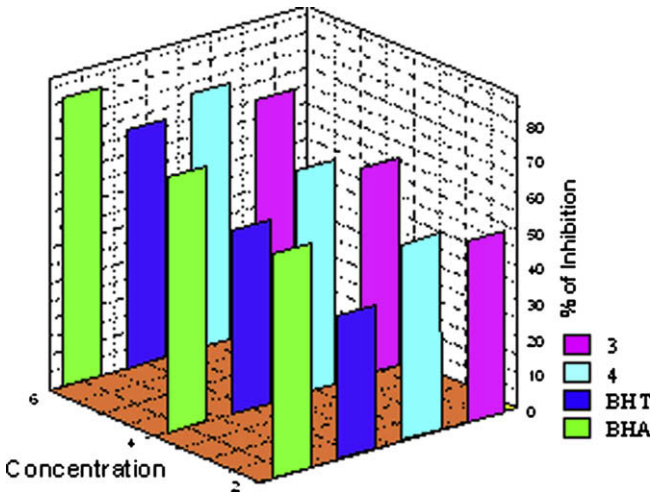

Fig. 8. Percentage of inhibition plot belongs to **3**/**4** for DPPH free radical scavenging activity at 20–60 μg/mL concentration with BHA, and BHT.

4.5. Antibacterial assay

The agar well diffusion method [64] was used for the assessment of antibacterial activity of the test samples. Medium (tryptone 10 g/l, yeast extract 5 g/l, sodium chloride 10 g/l, agar–agar 15 g/l, pH 7.2) was poured into sterilized Petri dishes (90 mm diameter). LB broth containing 100 μl of 24-h incubated cultures of the respective clinical isolates and the ATCC and MTCC strains was spread separately on the agar medium. Wells were created using a sterilized cork borer under aseptic conditions. Cell count was taken using heamocytometer after loading 10 μl of the cell suspension in PBS and no. of cells/mL was calculated, the final concentration of each strain was 106 cells/mL. Cultures were grown for 3 days at 37 °C and wells were made using cork borer and 100 μl (10 mg/mL) of test compounds was loaded to each wells. The reference antibacterial agent ciprofloxacin (10 μg/mL) was loaded in the corresponding wells. Plates were then incubated at 37 °C for 48 h. At the end of the incubation period, inhibition zones formed on the medium were evaluated in millimeters. The minimal inhibitory concentrations (MICs) of the newly synthesized compounds **3** and **4** were determined by microdilution techniques in LB broth, according to Clinical and Laboratory Standards Institute (CLSI), USA guidelines.

The bacterial inoculates were prepared in the same medium with density adjusted to a 0.5 McFarland turbidity standard colony

forming units and diluted 1:10 for the broth microdilution procedure. The microtiter plates were incubated at 37 °C and MIC was determined after 24 h of incubation. The highest activity of the standard drug compared with those of our synthesized compounds **3** and **4** indicated potent antibacterial activity (Table 5).

4.6. Bacterial strains

Of the six clinical strains three of the bacterial pathogens belongs to Gram-positive *S. aureus* – ATCC-29737, *B. subtilis* – NCIM-2010 and *S. pyogenes* – NCIM-2608 and Gram-negative bacteria such as *P. aeruginosa* – ATCC-20852, *K. pneumoniae* – MTCC-618 and *Escherichia coli* were collected from National Chemical Laboratory (NCL), Pune, India. All the bacterial microorganisms were maintained at −30 °C in Brain Heart Infusion (BHI) containing 17% (v/v) glycerol. Before testing, the suspensions were transferred to LB broth and cultured overnight at 37 °C. Inocula were prepared by adjusting the turbidity of the medium to match the 0.5 McFarland standards. Dilutions of this suspension in 0.1% peptone (w/v) solution in sterile water were inoculated on LB agar, to check the viability of the preparations.

4.6.1. Statistical analysis

The results of these experiments are expressed as mean ± S.E. of three replicates in each test. The data were evaluated by one-way analysis of variance (ANOVA) and mean separations were carried out using Duncan's Multiple Range Test [65] to assess the statistical significance. $P \leq 0.05$ was considered as statistically significant, using statistical software SPSS ver 11 (SPSS Inc., Chicago, USA).

4.7. DNA binding studies

4.7.1. Absorption spectroscopy

UV–vis spectra were recorded on a SHIMADZU, UV-1650 PC model spectrophotometer. Quartz cuvettes of 1 cm were used. The absorbance assessments were performed at pH 7.3 by keeping the concentration of DNA constant (0.25 mM), while varying the concentration of **3**/**4**. The values of the binding constants K_b were obtained according to the methods reported [66,67].

4.7.2. Viscosity measurements

Viscosity measurements were made according to semi-micro-dilution capillary viscometer (Viscomatic Fica MgW) with a thermostated bath D40S at 20 °C [68]. The flow time for water was 71.1 s. For viscosity experiments, samples of calf thymus DNA were sonicated [69] to fragments having an estimated molecular weight of approximately [70].

4.7.3. Thermal denaturation experiments

The DNA melting studies were done by controlling the temperature of the sample cell with a Shimadzu (SHIMADZU, UV-1650 PC) circulating bath while monitoring the absorbance at 260 nm. The temperature of the solution was continuously monitored with a thermo-couple attached to the sample holder.

Table 5
MIC (μg/mL) values of synthesized compounds **3** and **4**

Clinical strains	Minimal inhibitory concentrations (MIC)		
	Compound **3**	Compound **4**	Ciprofloxacin
Pseudomonas aeruginosa	16.0	16.0	6.25
Klebsiella pneumoniae	12.5	25.0	12.5
Escherichia coli	32	25.0	6.5
Staphylococcus aureus	11.0	8.0	6.75
Streptococcus pyogenes	12.5	12.5	6.25
Bacillus subtilis	16.25	16.25	12.5

4.8. In vitro antioxidant activity

4.8.1. Superoxide anion scavenging activity

Measurements of superoxide anion scavenging activity were based on the method described [71]. Superoxide radicals are generated in phenazine methosulfate (PMS)–NADH systems by oxidation of NADH and assayed by the reduction of nitroblue tetrazolium (NBT). In these experiments, the superoxide radicals were generated in 3 mL of Tris–HCl buffer (16 mM, pH 8.0) containing 1 mL of NBT (50 mM) solution, 1 mL NADH (78 mM) solution, and a sample solution of complexes (20, 40, 60 μg/mL) in ethanol. The reaction was started by adding 1 mL of phenazine methosulfate (PMS) solution (10 mM) to the mixture. The reaction mixture was incubated at 25 °C for 5 min and the absorbance was recorded at 560 nm. L-Ascorbic acid was used as a control. The percentage inhibition of superoxide anion generation was calculated using the formula shown in Eq. (1) [72].

$$\%\ \text{Inhibition} = \left[\frac{(A_0 \times A_1)}{A_0}\right] \times 100 \quad (1)$$

where A_0 was the absorbance of the control reaction and A_1 was the absorbance in the presence of samples **3** and **4**.

4.8.2. Scavenging of hydrogen peroxide

The ability of the scavenging effect of **3** and **4** to hydrogen peroxide was determined according to the reported method [73]. A solution of hydrogen peroxide (40 mM) was prepared in phosphate buffer (pH 7.4). Hydrogen peroxide concentration was determined spectrophotometrically from absorption at 230 nm. Complexes (20, 40, 60 μg/mL) in ethanol and distilled water were added to a hydrogen peroxide solution (0.6 mL, 40 mM). Absorbance of hydrogen peroxide at 230 nm was determined after 10 min against a blank solution. The percentage of scavenging of hydrogen peroxide was calculated using Eq. (1).

4.8.3. 1,1-Diphenyl-2-picryl-hydrazyl (DPPH) free radical scavenging activity

The free radical scavenging activity was measured against 1,1-diphenyl-2-picryl-hydrazyl (DPPH) using the method quoted by Refs. [74,75]. Briefly, 1 mL of 0.1 mM solution of DPPH in ethanol was added to 3 mL of ligands and complexes in phosphate buffer at different concentrations (20, 40, 60 μg/mL). The mixture was shaken vigorously and allowed to stand at room temperature for 30 min and then the absorbance was measured at 517 nm. The DPPH concentration (mM) in the reaction medium was calculated from the following calibration curve, determined by linear regression (R^2: 0.9769):

$$\text{Absorbance} = 104.09 \times \left[\text{DPPH}^*\right]$$

The DPPH radical concentration was calculated using the following Eq. (2):

$$\text{DPPH scavenging effect}\ (\%) = 100 - \left[\left(\frac{A_0 - A_1}{A_0}\right) \times 100\right] \quad (2)$$

where A_0 was the absorbance of the control reaction and A_1 was the absorbance in the presence of sample **3** or **4**.

4.8.4. Reducing power

The reducing power of **3** and **4** was determined according to the literature method [76]. The five concentrations of compounds (20, 40, 60 μg/mL) in 1 mL of distilled water were mixed with phosphate buffer (2.5 mL, 0.2 M, pH 6.6) and potassium ferricyanide [$K_3Fe(CN)_6$] (2.5 mL, 1%). The mixture was incubated at 50 °C for 20 min. A portion (2.5 mL) of trichloroacetic acid (10%) was added

to the mixture, which was then centrifuged for 10 min. The upper layer of the solution (2.5 mL) was mixed with distilled water (2.5 mL) and $FeCl_3$ (0.5 mL, 0.1%). The absorbance was measured at 700 nm.

Acknowledgment

One of the author Halehatty R. Prakash Naik is thankful to The Director, Sophisticated Instrumentation Facility Center, Indian Institute of Science, Bangalore, for the spectral facilities, University of Mysore for Elemental Analysis facility and SC/ST cell Kuvempu University for awarding Junior Research Fellowship (JRF).

References

[1] R.D. Larsen, E.G. Corley, A.O. King, J.D. Carrol, P. Davis, T.R. Verhoeven, P.J. Reider, M. Labelle, J.Y. Gauthier, Y.B. Xiang, R.J. Zamboni, J. Org. Chem. 61 (1996) 3398–3405.
[2] G. Roma, M.D. Braccio, G. Grossi, F. Mattioli, M. Ghia, Eur. J. Med. Chem. 35 (2000) 1021–1035.
[3] Y.L. Chen, K.C. Fang, J.Y. Sheu, S.L. Hsu, C.C. Tzeng, J. Med. Chem. 44 (2001) 2374–2377.
[4] D. Dube, M. Blouin, C. Brideau, C.C. Chan, S. Desmarais, D. Ethier, J.P. Falgueyret, R.W. Friesen, M. Girard, Y. Girard, J. Guay, D. Riendeau, P. Tagari, R.N. Young, Bioorg. Med. Chem. Lett. 8 (1998) 1255–1261.
[5] M.P. Maguire, K.R. Sheets, K. McVety, A.P. Spada, A. Zilberstein, J. Med. Chem. 37 (1994) 2129–2141.
[6] M. Iwaoka, S. Tomoda, J. Am. Chem. Soc. 116 (1994) 2557–2564.
[7] T. Saiki, K. Goto, R. Okazaki, Angew. Chem., Int. Ed. Engl. 36 (1997) 2223–2235.
[8] T.C. Stadtman, Annu. Rev. Biochem. 49 (1980) 93–110.
[9] D.L. Klayman, W.H. Güther (Eds.), Organic Selenium Compounds: Their Chemistry and Biology, John Wiley and Sons, Inc, New York, 1973.
[10] J.E. Spallholz, Free Radical Biol. Med. 17 (1994) 45–64.
[11] O.E. Olson, J. Am. Coll. Toxicol. 5 (1986) 45–70.
[12] L. Fishbein, Toxicol. Environ. Chem. 12 (1986) 1–30.
[13] W. Insel, Perspectives in Nutrition, Mosby, New York, 1996, pp. 396–570.
[14] J.V. Vadagama, Y. Wu, D. Shen, S. Hisa, J. Block, Anticancer Res. 29 (2000) 1391–1414.
[15] T. Tanaka, B.S. Reddy, K. El-Bayoumy, Jpn. J. Cancer Res. 76 (1985) 462–467.
[16] D. Chattopadhyay, G. Arunachalam, A.B. Mandal, T.K. Sur, S.C. Mandal, S.K. Bhattacharya, J. Ethnopharmacol. 82 (2002) 229–237.
[17] G.S. Sidhu, H. Mani, J.P. Gaddipatti, A.K. Singh, P. Seth, K.K. Banaudha, G.K. Patnaik, R.K. Maheshwari, Wound Repair Regen. 7 (1999) 362–374.
[18] E. Aliyeva, S. Umur, E. Zafer, G. Acigoz, Biomaterials 25 (2004) 4633–4637.
[19] B.M. Baboir, New Engl. J. Med. 298 (1978) 629–668.
[20] K.K. Griendling, Circ. Res. 86 (2000) 494–501.
[21] B. Thiem, O. Grosslinka, Fitoterapia 75 (2003) 93–95.
[22] P.W. Thulstrup, T. Thormann, Biochem. Biophys. Res. Commun. 254 (1999) 416–421.
[23] D. Mark, E.R. Hutchenson, I.F. Cheng, J. Agric. Food Chem. 53 (2005) 2953–2960.
[24] T. Walle, T.S. Vincent, U.K. Walle, Biochem. Pharmacol. 65 (2003) 1603–1610.
[25] M. Lodovici, M. Guglielmi, P.D. Meoni, Food Chem. Toxicol. 39 (2001) 1205–1210.
[26] C.W. Lonneke, C.H. Hollman, A.W. Boots, J.C.S. Kleeinjans, Mutat. Res. 582 (2005) 155–162.
[27] Z.H. Skraup, Monatsh. Chem. 2 (1881) 139–154.
[28] O. Doebner, W. Von Miller, Chem. Ber. 17 (1884) 1698–1708.
[29] B.E. Cohn, R.G. Gustavson, J. Am. Chem. Soc. 50 (1928) 2709–2718.
[30] F.L. Warren, J. Chem. Soc. (1936) 1366–1378.
[31] O. Peters, W. Friedrichsen, Tetrahedron Lett. 36 (1995) 8581–8582.
[32] E.C. Riesgo, X. Jin, R.P. Thummel, J. Org. Chem. 61 (1996) 3017–3025.
[33] O. Meth-Cohn, B. Narine, B. Tarnowski, J. Chem. Soc., Perkin Trans. 1 (1981) 1520–1526.
[34] O. Meth-Cohn, Heterocycles 35 (1993) 539–546.
[35] Y.L. Janin, E. Bisagni, D. Carrez, J. Heterocycl. Chem. 30 (1993) 1129–1138.
[36] B.C. Baguley, L. Zhuang, E.M. Marshall, Cancer Chemother. Pharmacol. 36 (1995) 244–256.
[37] J.A. Spicer, S.A. Gamage, G.J. Atwell, G.J. Finlay, B.C. Baguley, W.A. Denny, J. Med. Chem. 40 (1997) 1919–1928.
[38] B.P. Nandeshwarappa, D.B. Aruna Kumar, M.N. Kumaraswamy, Y.S. Ravi Kumar, H.S. Bhojya Naik, K.M. Mahadevan, Phosphorus Sulfur Silicon Relat. Elem. 181 (2006) 1545–1556.
[39] M.C. Prabhakara, H.S. Bhojya Naik, V. Krishna, H.M. Kumaraswamy, Nucleosides Nucleotides Nucleic Acids 26 (2007) 459–471.
[40] M.C. Prabhakara, B. Basaavaraju, H.S. Bhojya Naik, Bioinorg. Chem. Appl. (2007) 36497 7p.
[41] T.R. Ravikumar Naik, H.S. Bhojya Naik, M. Raghavendra, S.R. Gopalkrishna Naik, Arkivoc XV (2006) 84–94.
[42] T.R. Ravikumar Naik, H.S. Bhojya Naik, S.R. Gopala Krishna Naik, J. Sulfur Chem. 28 (2007) 393–400.
[43] G.P. Bharath (Ed.), Practical Manual for Pharmaceutics, Sunitha Publishers, Shimoga – Karnataka – India, 1996, pp. 108–109.
[44] R. Scherrer, P. Gerhardt, J. Bacteriol. 107 (1971) 718–735.
[45] J.E.C. Betoni, R.P. Mantovani, L.N. Barbosa, L.C. Di Stasi, J.A. Fernandes, Memórias do Instituto Oswaldo, Rio de Janeiro 101 (2006) 387–390.
[46] V. Nikaido, Microbiol. Rev. 1 (1985) 1–32.
[47] D. Freifelder (Ed.), Physical Biochemistry, W.H. Freeman and Company, New York, 1976.
[48] J.B. Lambert, H.F. Shurvell, D.A. Lightner, R.G. Cooks (Eds.), Organic Structural Spectroscopy, Prentice-Hall, Inc, New Jersey, 1998.
[49] B. Allard, M. Jouini, G.A. Bistocchi, P.L. Orvietani, A. Ricci, E. Lescot, A. Schwaller, J. Chem. Res. (1995) 1314–1321.
[50] S.L. Mee, A. Pierre, J. Markovits, G. Atassi, A.J. Sablon, J.M. Saucier, Mol. Pharmacol. 53 (1998) 213–221.
[51] M. Maiti, R. Nandi, K. Chauduri, Indian J. Biochem. Biophys. 21 (1984) 158–162.
[52] L. Laure, R. Christian, M. Gabriel, C. Paoletti, E. Bisagni, J. Paoletti, J. Med. Chem. 31 (1988) 1951–1963.
[53] D.J. Patel, Acc. Chem. Res. 12 (1979) 118–124.
[54] G.L. Zuby, Biochemistry, second ed. McMillan, New York, 1988, p. 236.
[55] A. McCoubery, H.C. Latham, P.R. Cook, A. Rodger, G. Lowe, FEBS Lett. 73 (1996) 380–387.
[56] R.J. Ruch, S.J. Cheng, J.E. Klaunig, Carcinogenesis 10 (1989) 1003–1008.
[57] S. Meir, J. Kanner, B. Akiri, S.P. Hadas, J. Agric. Food Chem. 43 (1995) 1813–1815.
[58] P.D. Duh, Y.Y. Tu, G.C. Yen, Lebensm. Wiss. Technol. 32 (1999) 269–277.
[59] L.W. Chang, W.J. Yen, S.C. Huang, P.D. Duh, Food Chem. 78 (2002) 347–354.
[60] I. Gulcin, M.E. Buyukokuroglu, M. Oktay, O.I. Kufrevioglu, J. Pineal Res. 33 (2002) 167–171.
[61] T.K. Chatterjee, A. Chakravorty, Indian Drugs 30 (1993) 450–452.
[62] C. Pandarinathan, G.B. Sajithal, G. Chandrakasan, Indian J. Exp. Biol. 36 (1998) 896–902.
[63] J.F. Woessner, Biochem. Biophys. 93 (1961) 440–447.
[64] D. Udupa, R. Kulkarni, S.L. Udupa, Int. J. Pharm. 33 (1995) 37–40.
[65] P.K. Mukherjee, R. Balasubramanian, K. Saha, B.P. Saha, Indian Drugs 32 (1995) 274–276.
[66] J.J. Stephanos, J. Inorg. Biochem. 62 (1996) 155–169.
[67] W. Zhong, Y. Wang, J.S. Yu, Y. Liang, K. Ni, S. Tu, J. Pharm. Sci. 93 (2004) 1039–1046.
[68] A. Baez, F.A. Gonzalez, D. Vazquez, M. Waring, Biochem. Pharmacol. 32 (1983) 2089–2094.
[69] G. Cohen, H. Eisenberg, Biopolymers 8 (1969) 45–55.
[70] D.M. Crothers, B.H. Zimm, J. Mol. Biol. 12 (1965) 525–529.
[71] I. Gulcin, M. Oktay, E. Kirecci, O.I. Kufrevioglu, Food Chem. 83 (2003) 371–382.
[72] X.Y. Ye, H.X. Wang, F. Liu, T.B. Ng, J. Biochem. Cell Biol. 32 (2000) 235–241.
[73] K. Shimada, K. Fujikawa, K. Yahara, T. Nakamura, J. Agric. Food Chem. 40 (1992) 945–948.
[74] J. Bernadou, G. Pratviel, F. Bennis, M. Girardet, B. Meunier, Biochemistry 28 (1989) 7268–7275.
[75] I. Gulcin, M. Uguz, M. Oktay, S. Beydemir, O.I. Kufrevioglu, J. Food Technol. 1 (2003) 9–16.
[76] I. Gulcin, M.E. Buyukokuroglu, M. Oktay, O.I. Kufrevioglu, J. Ethnopharmacol. 86 (2003) 51–58.